Fault Locating From DFR Data: Effects of Grounding, Asymmetry and Arc Voltage on Accuracy

A. P. Sakis Meliopoulos
School of Electrical and Computer Engineering
Georgia Institute of Technology
Atlanta, GA 30332-0250
Sakis.meliopoulos@ece.gatech.edu

George J. Cokkinides
Department of Electrical Engineering
University of South Carolina
Columbia, SC 29208
cokk@engr.sc.edu

Abstract: Fault locating has become a standard algorithm of numerical relays and fault recording equipment. At the same time, present algorithms have several shortcomings. The most serious are: (a) difficulties in handling and accounting for the arc voltage, (b) difficulties in modeling the impedance of the fault return path and (c) difficulties in handling instrumentation errors. This paper provides an in depth analysis of these problems and presents three classes of algorithms for fault locating. The three classes of algorithms correspond to the type of technology and available information from fault recorders: (a) single end data, (b) double end synchronized data, and (c) double end unsynchronized data. The algorithms account for arc voltage, fault current return path impedance, impedance asymmetry of three phase systems and circuit grounding impedances. The numerical experiments quantify the effect of these factors on fault locating accuracy. It is shown that use of line asymmetric models drastically improves the accuracy of the algorithms. The proposed algorithms operate on DFR data available from commercially available fault recorders and they require physical data of the faulted circuit that are readily available.

1.0 Introduction

The problem of fault locating in power circuits has been long ago recognized as an important one for two reasons: (a) minimization of downtime by quick repair and therefore increased system reliability (especially for cable circuits) and (b) improved selectivity of protection schemes by virtue of knowledge of fault location (for example distance relays are based on evaluation of the fault distance). Recent trends towards automation have accentuated the importance of fault locating. Over the years, several technologies for fault locating have been developed. These technologies can be categorized into the following:

Use of thumpers to locate a cable fault
Use of Faulted Circuit Indicators
Use of traveling waves method to determine the fault distance
Use of fault current and voltage to compute distance to fault

The first two methods are extensively used in distribution circuits, especially on URD cable systems. The thumper technology consists of injecting an impulse to the faulted cable. The fault in the cable is reignited under the impulse and the generated noise is utilized to determine the location of the fault. Application of the thumper requires that the cable is out of service and in general it is time consuming. A criticism of the thumper technology is that it subjects the cable to additional surges and therefore may affect the life of the cable. The faulted circuit indicators are devices which are triggered by the flow of the fault current. Basically, a faulted circuit indicator is a two state device: state one is normal and state two indicates that an electric current has been detected which was above the threshold value. Application of many faulted circuit indicators at strategic locations along a circuit, i.e. one at each transformer, provides means for determining the location of the fault between two locations. Models with manual or automatic reset are available.

The third method requires dedicated equipment to measure the travel time to the fault. The travel time is used to extract the distance to the fault from the known speed of propagation of EM waves on the circuit. Specifically, the travel time from the monitoring location to the fault is measured with rather sophisticated hardware. For a given cable parameters the speed of propagation of surges along the cable is known and is utilized to estimate the location of the fault. This technology is complex, requiring sophisticated and expensive hardware.

The forth method requires recording of voltages and currents at any location along the faulted circuit. From the recorded voltages and currents and the known impedance per unit length of the system, the distance to the fault can be estimated. Recently, the introduction of inexpensive microcontrollers, numerical relays and digital fault recording equipment have made the last method very attractive. Specifically, the mentioned equipment provides recordings of the voltage and current during fault. These recordings are typically stored and/or can be transmitted to central locations via a variety of communication media, i.e. telephone, fiber, microwave, etc. The data are processed to estimate the distance to the fault.

The technology that is described in this paper is based on statistical estimation methods applied on recorded current and voltage data during a fault. Specifically, the method is based on a detailed model of the faulted circuit that accounts for asymmetry, grounding impedances and arc voltage. The objective of the present paper is to study the impact of various commonly used approximations on the accuracy of the fault locating algorithms.
This paper is organized as follows: Section 2 describes the basic approach to fault locating from recordings of fault data and the factors affecting the accuracy of the methods. Section 3 describes the proposed algorithms. Section 4 discusses the implementation and numerical experiments that quantify the effects of various simplifying assumptions on the accuracy of

fault locating algorithms. Section 5 provides a discussion of the main findings and section 6 provides the conclusions.

2.0 Factors Affecting Fault Distance Estimation Algorithms

Fault locating algorithms using fault recordings are based on the observation that the recorded voltage is a function of the distance of the fault from the recording device, the impedance of the circuit per unit length and the fault current. Specifically, one can write:

$$v(t) = M(\ell)i(t) + Nv_{arc}(t) \qquad (1)$$

where:

v(t) is the vector of recorded voltages
i(t) is the vector of recorded currents
$M(\ell)$ is an impedance operator that dependson the fault distance
$v_{arc}(t)$ is the arc voltage
N is a matrix that depends on the fault type (single phase, double line, etc.)

For power circuits the impedance operator as a function of fault location can be accurately determined. However, in most algorithms, simplifying assumptions are introduced, for example, the impedance operator is computed from positive, negative and zero sequence impedances. This particular simplification introduces errors in the impedance operator that may impact the accuracy of fault locating. Other effects, for example variations of the impedance due to grounding and earth effects are small for effectively grounded system but can be substantial for other systems. Variations of circuit resistance due to temperature changes can be also significant, especially for cable systems. In addition, the precision of the recorded voltages and currents plays an important role as well as the duration of the recorded data. A theoretical investigation of the possible sources of error was performed some time ago. The investigation has identified the following error sources grouped into two categories:

Category A: Data Acquisition Errors: (1) Potential device inaccuracies, (2) Current transformer inaccuracies, (3) Discretization error from A/D conversion, and (4) Aliasing of digitized measurements

Category B: Algorithmic Errors: (1) Arc voltage distortion and uncertainty, (2) Circuit asymmetry among phases, (3) Circuit grounding impedance uncertainty, (4) Fault current and voltage DC offset, (5) Power frequency harmonics, (6) Induced voltages from nearby circuits, (7) Random noise (arcing, transients, etc), (8) Duration of short circuit current

In this paper we focus on the algorithmic errors and in particular on three specific sources of error: (a) circuit asymmetry, (b) circuit grounding and (c) arc voltage. We propose a series of fault locating algorithms that precisely model these parameters. These algorithms are used to quantify the effect of these sources of error on the accuracy of the fault locating process.

3.0 Proposed Approach

The impact of the various parameters on fault locating accuracy can be determined by appropriate models that account for these effects. Specifically, one can perform numerical experiments with complete models and compare the results with the usual simplified models. In this section we present the detailed models used for this investigation. Specifically we present three models/algorithms that correspond to (a) single end data, (b) double end synchronized data, and (c) double end non-synchronized data. For each one of the cases, an appropriate simplifying assumption will generate the usual simplified models. In order to quantify the accuracy of the commercially available fault locating algorithms, all of the above algorithms have implemented to operate on phasors of the recorded data.

3.1 Single End Data

A set of algorithms are described for the case in which data is available only at one end of the faulted circuit.

3.1.1 Detailed Line and Fault Model

Assume that fault data has been recorded at Bus 1 of a line of total length L during a fault at some point of the line (ℓ miles from Bus 1) as it is illustrated in Figure 1. The fault recorder (DFR) or relay or IED has captured the voltage and current waveforms at all three phases at the Bus 1 terminal.

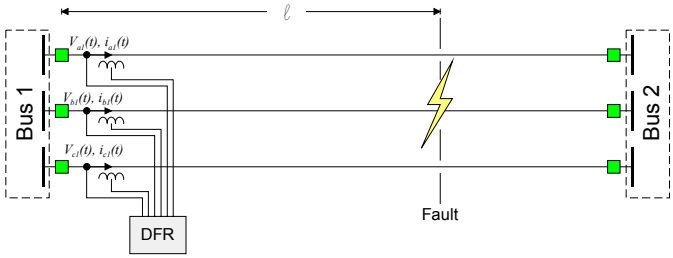

Figure 1. A Faulted Power Line with a DFR at One Terminal Only

The detailed model is based on an estimation technique and uses all recorded data (both faulted and un-faulted phase voltages and currents). For this purpose the equations are cast in matrix form using the voltage and current notation introduced in Figure 2.
Based on this notation, the following equations can be written:

$$\begin{bmatrix} \tilde{I}_1 \\ \tilde{I}_3 \end{bmatrix} = Y_A(l) \begin{bmatrix} \tilde{V}_1 \\ \tilde{V}_3 \end{bmatrix},$$

$$\tilde{I}_5 = Y_F \tilde{V}_3$$

where:

$$Y_A(l) = \begin{bmatrix} \frac{1}{\ell} Y_{SERA} + \ell Y_{SHA} & -\frac{1}{\ell} Y_{SERA} \\ -\frac{1}{\ell} Y_{SERA} & \frac{1}{\ell} Y_{SERA} + \ell Y_{SHA} \end{bmatrix}$$

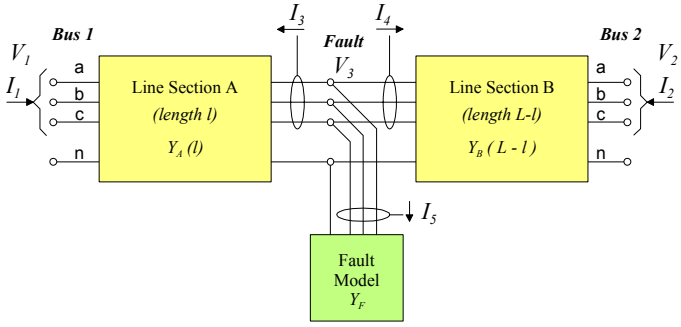

Figure 2. Definition of Measured Voltages and Currents

and Y_F depends on the fault type. For example for a phase A to neutral fault and a phase A to C fault, the respective matrices are:

$$Y_F = g\begin{bmatrix} 1 & 0 & 0 & -1 \\ 0 & 0 & 0 & 0 \\ 0 & 0 & 0 & 0 \\ -1 & 0 & 0 & 1 \end{bmatrix}, \text{ and } Y_F = g\begin{bmatrix} 1 & 0 & -1 & 0 \\ 0 & 0 & 0 & 0 \\ -1 & 0 & 1 & 0 \\ 0 & 0 & 0 & 0 \end{bmatrix}$$

The fault conductance is assumed to be current dependent in accordance to Harrington's model:

$$\frac{dg(t)}{dt} = \frac{1}{\tau}\left(\frac{i_f^2(t)}{P_0} - g(t)\right)$$

where: g is the arc conductivity
i is the arc current
τ is a time constant related to arc dynamics, and
P_0 is a constant related to the air gap length

The above differential equation is converted into an approximate equation of the form:

$$g = \frac{I_f^2}{P_0}$$

Note that Y_{SERA}, Y_{SHA} are the per-unit length series and shunt components extracted from the line full (exact) admittance matrix. Specifically, these matrices are computed as follows:

$$Y_{SERA} = -L\,Y_{12}$$
$$Y_{SHA} = \frac{1}{L}\left(Y_{11} + Y_{12}\right)$$

where Y_{11}, Y_{12} are the two upper blocks of the exact line admittance matrix. Note that, initially, it is assumed that $Y_{ser1} = Y_{ser2}$ and $Y_{sh1} = Y_{sh2}$. Once the first fault distance estimate is computed, the solution is refined by re-computing these matrices for line length ℓ, and repeating the fault distance computations:

$$Y_{SERA} = -\ell\,Y_{12}(\ell)$$
$$Y_{SHA} = \frac{1}{\ell}\left(Y_{11}(\ell) + Y_{12}(\ell)\right)$$

3.1.2 Matrix Formulation

We define as state vector the union of the following two subvectors:

$x_1^T = [V_1, \ell, g]$, and $x_2^T = [V_3, x, y]$

Define the measurement vector z as follows:

$z_1^T = [I_1^m, V_1^m, g, V_{n1}, V_{n2}]$

Using the above state and measurement vector definitions, the linearized system of the model equations is written in compact matrix notation as follows:

$z = H_1 x_1 + H_2 x_2 - b + r$

$0 = K_1 x_1 + K_2 x_2 - c$

The optimization solution is computed as follows. Solving constraint equation for x2:

$x_2 = K_2^{-1}(c - K_1 x_1)$

Substituting x2 in the measurement equation:

$z = H_1 x_1 + H_2 K_2^{-1}(c - K_1 x_1) - b + r$

or :

$z = (H_1 - H_2 K_2^{-1} K_1)\, x_1 + H_2 K_2^{-1} c - b + r$

let $H = H_1 - H_2 K_2^{-1} K_1$,
and $d = z + b - H_2 K_2^{-1} c$

then the optimization result is:

$x_1 = (H^T W H)^{-1} H^T W d$
$x_2 = K_2^{-1}(c - K_1 x_1)$

3.1.3 Solution Algorithm

The solution algorithm is as follows:

1. Assume an initial value for the state, for example the initial gues of the fault distance is assumed to be half of the line length.
2. Compute Matrices H1, H2, K1, K2, and Vectors b and c at operating point.
3. Update states x_1, x_2 as follows:

$x_1 = (H^T WH)^{-1} H^T W d$
$x_2 = K_2^{-1} (c - K_1 x_1)$
where:
$H = H_1 - H_2 K_2^{-1} K_1$
$d = z + b - H_2 K_2^{-1} c$

4. Compute Residual Norm oink ρ as follows:
$\rho = || z + b - H_1 x_1 - H_2 x_2 ||$ and if $\Delta\rho < \varepsilon_1$ Stop, otherwise go to step 2.

3.1.4 Simulation of Asymmetry, Grounding and Arc Effects

The described model can be used to evaluate the impact of asymmetry, grounding and arc effects on the accuracy of fault locating. For this purpose, the model described above can be "forced" to (a) ignore asymmetry, (b) ignore grounding, (c) ignore the arc voltage or any combination of the above. For example, in order to ignore the arc voltage it is sufficient to set the variable g equal to zero. In order to ignore the transmission tower grounds it is sufficient to set the tower grounds equal to a small value, i.e. 0.1 ohms. Or in order to ignore asymmetry, the line matrices are computed from the positive, negative and zero sequence impedances.

3.2. Double End Synchronized Data

A set of algorithms are described for the case in which data is available at both ends of the faulted circuit and the data is GPS synchronized, i.e. synchronized with precision better than one microsecond.

3.2.1 Detailed Line and Fault Model

Assume that fault data has been recorded at both ends of a line of total length L during a fault at some point of the line (ℓ miles from Bus 1) as it is illustrated in Figure 3. Let's consider the case that the measurements are GPS synchronized. The fault recorders (DFRs) or relays or IEDs have captured the voltage and current waveforms at all three phases of both line terminals (Bus 1 and Bus 2).

The detailed model is based on an estimation technique and uses all recorded data (both faulted and un-faulted phase voltages and currents). For this purpose the equations are cast in matrix form using the voltage and current notation introduced in Figure 2.

Based on this notation, the following equations can be written:

$$\begin{bmatrix} \tilde{I}_1 \\ \tilde{I}_3 \end{bmatrix} = Y_A(l) \begin{bmatrix} \tilde{V}_1 \\ \tilde{V}_3 \end{bmatrix},$$

$$\begin{bmatrix} \tilde{I}_2 \\ \tilde{I}_4 \end{bmatrix} = Y_B(L-l) \begin{bmatrix} \tilde{V}_2 \\ \tilde{V}_3 \end{bmatrix},$$

$$\tilde{I}_5 = Y_F \tilde{V}_3$$

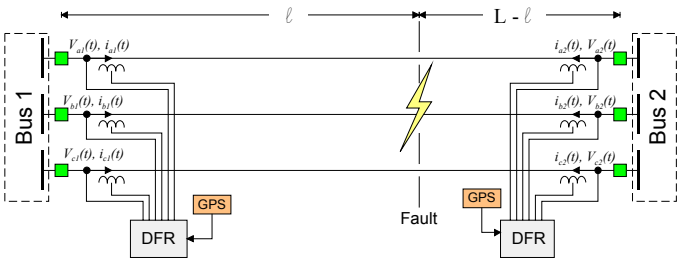

Figure 3. A Faulted Power Line with GPS Synchronized DFRs at Both Terminals

where:

$$Y_A(l) = \begin{bmatrix} \frac{1}{\ell} Y_{SERA} + \ell Y_{SHA} & -\frac{1}{\ell} Y_{SERA} \\ -\frac{1}{\ell} Y_{SERA} & \frac{1}{\ell} Y_{SERA} + \ell Y_{SHA} \end{bmatrix}$$

$$Y_B(l) = \begin{bmatrix} \frac{1}{L-\ell} Y_{SERB} + (L-\ell) Y_{SHB} & -\frac{1}{L-\ell} Y_{SERB} \\ -\frac{1}{L-\ell} Y_{SERB} & \frac{1}{L-\ell} Y_{SERB} + (L-\ell) Y_{SHB} \end{bmatrix}$$

and Y_F depends on the fault type as it has been described in the previous case.

Note that Y_{SERA}, Y_{SERB}, Y_{SHA}, Y_{SHB} are the per-unit of length series and shunt components extracted from the line full (exact) admittance matrix. Specifically, these matrices are computed as follows:

$$Y_{SERA} = Y_{SERB} = -L Y_{12}$$

$$Y_{SHA} = Y_{SHB} = \frac{1}{L}\left(Y_{11} + Y_{12}\right)$$

where Y_{11}, Y_{12} are the two upper blocks of the exact line admittance matrix. Note that, initially, it is assumed that $Y_{ser1} = Y_{ser2}$ and $Y_{sh1} = Y_{sh2}$. Once the first fault distance estimate is computed, the solution is refined by re-computing these matrices for line lengths ℓ and $L - \ell$, and repeating the fault distance computations:

$$Y_{SERA} = -\ell Y_{12}(\ell), \quad Y_{SERB} = (\ell - L) Y_{12}(L - \ell)$$

$$Y_{SHA} = \frac{1}{\ell}\left(Y_{11}(\ell) + Y_{12}(\ell)\right),$$

$$Y_{SHB} = \frac{1}{L-\ell}\left(Y_{11}(L-\ell) + Y_{12}(L-\ell)\right)$$

Expanding equation (1) using the above notation yields:

$I_1 = (1/\ell)\ Y_{SERA}\ V_1 + \ell Y_{SHA}\ V_1 - (1/\ell)\ Y_{SERA}\ V_3$

$I_2 = 1/(L-\ell)\ Y_{SERB}\ V_2 + (L-\ell)\ Y_{SHB}\ V_2 - 1/(L-\ell)\ Y_{SERB}\ V_3$

$I_3 = -(1/\ell)\ Y_{SERA}\ V_{1+}\ (1/\ell)\ Y_{SERA}\ V_3 + \ell Y_{SHA}\ V_3$

$I_4 = -(1/L-\ell)\ Y_{SERB}\ V_{2+}\ (1/L-\ell)\ Y_{SERB}\ V_3 + (L-\ell)\ Y_{SHB}\ V_3$

$I_5 = g\ Y_F\ V_3$

Kirchoff's law at the fault location yields:

$I_3 + I_3 + I_3 = 0$, or

$0 = gY_F\ V_3 - (1/\ell)Y_{SERA}\ V_1 + (1/\ell)\ Y_{SERA}V_3 + \ell Y_{SHA}V_3 - (1/L-\ell)Y_{SERB}V_2 + (1/L-\ell)Y_{SERB}V_3 + (L-\ell)Y_{SHB}\ V_3$

The above equations are "qudratized", i.e. with the addition of new variables, the equations are expressed in terms of linear terms and few quadratic terms. The final result includes the following state vector.

$x^T = [V_1, V_2, \ell, g, | V_3, x, y]$

and the measurement vector is:

$z_1^T = [I_1^m, I_2^m, V_1^m, V_2^m, g, V_{n1}, V_{n2}]$

3.2.2 Matrix Formulation

The state vector is partitioned as follows:

$x_1^T = [V_1, V_2, \ell, g]$, and $x_2^T = [V_3, x, y]$

Define the measurement vector z as follows:

$z_1^T = [I_1^m, I_2^m, V_1^m, V_2^m, g, V_{n1}, V_{n2}]$

Using the above state and measurement vector definitions, the linearized system of cat equations (7) is written in compact matrix notation as follows:

$z = H_1 x_1 + H_2 x_2 - b + r$

$0 = K_1 x_1 + K_2 x_2 - c$

The optimization solution is computed as follows. Solving constraint equation for x2:

$x_2 = K_2^{-1} (c - K_1 x_1)$

Substituting x2 in the measurement equation:

$z = H_1 x_1 + H_2 K_2^{-1} (c - K_1 x_1) - b + r$

or :

$z = (H_1 - H_2 K_2^{-1} K_1)\ x_1 + H_2 K_2^{-1} c - b + r$

let $H = H_1 - H_2 K_2^{-1} K_1$,
and $d = z + b - H_2 K_2^{-1} c$

then the optimization result is:

$x_1 = (H^T WH)^{-1} H^T W d$
$x_2 = K_2^{-1} (c - K_1 x_1)$

3.2.3 Solution Algorithm

The Solution algorithm is as follows:

1. Compute approximate solution using method described in section 3.1
2. Compute Matrices H1, H2, K1, K2, and Vectors b and c at operating point.
3. Update states x_1, x_2 as follows:

   $x_1 = (H^T WH)^{-1} H^T W d$
   $x_2 = K_2^{-1} (c - K_1 x_1)$
   where:
   $H = H_1 - H_2 K_2^{-1} K_1$
   $d = z + b - H_2 K_2^{-1} c$

4. Compute Residual Norm oink ρ as follows:
   $\rho = || z + b - H_1 x_1 - H_2 x_2 ||$ and if $\Delta\rho < \varepsilon_1$ Stop, otherwise go to step 2.

3.2.4 Simulation of Asymmetry, Grounding and Arc Effects

The described model can be used to evaluate the impact of asymmetry, grounding and arc effects on the accuracy of fault locating. For this purpose, the model described above can be "forced" to (a) ignore asymmetry, (b) ignore grounding, (c) ignore the arc voltage or any combination of the above. For example, in order to ignore the arc voltage it is sufficient to set the variable g equal to zero. In order to ignore the transmission tower grounds it is sufficient to set the tower grounds equal to a small value, i.e. 0.1 ohms. Or in order to ignore asymmetry, the line matrices are computed from the positive, negative and zero sequence impedances.

3.3. Double End Un-Synchronized Data

A set of algorithms are described for the case in which data is available at both ends of the faulted circuit and the data is non synchronized, i.e. there is appreciable and unknown time difference between the data at the two ends.

3.3.1 Detailed Line and Fault Model

Assume that fault data has been recorded at both ends of a line of total length L during a fault at some point of the line (ℓ miles from Bus 1) as it is illustrated in Figure 4.1. Let's consider the case that the measurements are un-synchronized. The fault recorders or relays (DFRs) have captured the voltage and current waveforms at all three phases of both line terminals (Bus 1 and Bus 2).

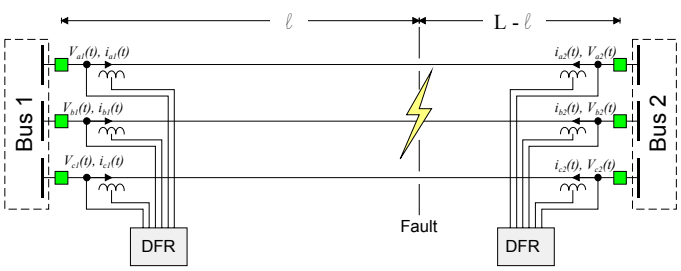

Figure 4. A Faulted Power Line with Unsynchronized DFRs at Both Terminals

The detailed model is based on an estimation technique using the same circuit model as for the double end synchronized data case. Refer to section 3.2 for details. The only difference is that the measurements on one side are time shifted by the sampling time skew at the two line ends. The time skew is represented by the phasor $e^{j\alpha}$. Specifically, the equations are cast in matrix form using the voltage and current notation introduced in Figure 2.

Based on this notation, the following equations can be written:

$$\begin{bmatrix} \tilde{I}_1 \\ \tilde{I}_3 \end{bmatrix} = Y_A(l) \begin{bmatrix} \tilde{V}_1 \\ \tilde{V}_3 \end{bmatrix},$$

$$\begin{bmatrix} \tilde{I}_2 e^{j\alpha} \\ \tilde{I}_4 \end{bmatrix} = Y_B(L-l) \begin{bmatrix} \tilde{V}_2 e^{j\alpha} \\ \tilde{V}_3 \end{bmatrix},$$

$$\tilde{I}_5 = Y_F \tilde{V}_3$$

where:

$$Y_A(l) = \begin{bmatrix} \frac{1}{\ell} Y_{SERA} + \ell Y_{SHA} & -\frac{1}{\ell} Y_{SERA} \\ -\frac{1}{\ell} Y_{SERA} & \frac{1}{\ell} Y_{SERA} + \ell Y_{SHA} \end{bmatrix}$$

$$Y_B(l) = \begin{bmatrix} \frac{1}{L-\ell} Y_{SERB} + (L-\ell) Y_{SHB} & -\frac{1}{L-\ell} Y_{SERB} \\ -\frac{1}{L-\ell} Y_{SERB} & \frac{1}{L-\ell} Y_{SERB} + (L-\ell) Y_{SHB} \end{bmatrix}$$

and Y_F depends on the fault type, as described in the previous case.

Note that Y_{SERA}, Y_{SERB}, Y_{SHA}, Y_{SHB} are the per-unit of length series and shunt components extracted from the line full (exact) admittance matrix. Specifically, these matrices are computed as follows:

$$Y_{SERA} = Y_{SERB} = -L\, Y_{12}$$

$$Y_{SHA} = Y_{SHB} = \frac{1}{L}\left(Y_{11} + Y_{12}\right)$$

where Y_{11}, Y_{12} are the two upper blocks of the exact line admittance matrix. Note that, initially, it is assumed that $Y_{ser1} = Y_{ser2}$ and $Y_{sh1} = Y_{sh2}$. Once the first fault distance estimate is computed, the solution is refined by re-computing these matrices for line lengths l and L-l, and repeating the fault distance computations:

$$Y_{SERA} = -\ell\, Y_{12}(\ell), \quad Y_{SERB} = (\ell - L)\, Y_{12}(L-\ell)$$

$$Y_{SHA} = \frac{1}{\ell}\left(Y_{11}(\ell) + Y_{12}(\ell)\right), \quad Y_{SHB} = \frac{1}{L-\ell}\left(Y_{11}(L-\ell) + Y_{12}(L-\ell)\right)$$

Expanding equation (1) using the above notation yields:

$I_1 = (1/\ell)\, Y_{SERA}\, V_1 + \ell Y_{SHA}\, V_1 - (1/\ell)\, Y_{SERA}\, V_3$

$I_2 = 1/(L-\ell)\, Y_{SERB}\, V_2 + (L-\ell)\, Y_{SHB}\, V_2 - 1/(L-\ell)\, Y_{SERB}\, V_3$

$I_3 = -(1/\ell)\, Y_{SERA}\, V_1 + (1/\ell)\, Y_{SERA}\, V_3 + \ell Y_{SHA}\, V_3$

$I_4 = -(1/L-\ell)\, Y_{SERB}\, V_2 + (1/L-\ell)\, Y_{SERB}\, V_3 + (L-\ell)\, Y_{SHB}\, V_3$

$I_5 = g\, Y_F\, V_3$

Kirchoff's law at the fault location yields:

$I_3 + I_3 + I_3 = 0$, or

$0 = gY_F\, V_3 - (1/\ell) Y_{SERA}\, V_1 + (1/\ell)\, Y_{SERA} V_3 + \ell Y_{SHA} V_3 - (1/L-\ell) Y_{SERB} V_2 + (1/L-\ell) Y_{SERB} V_3 + (L-\ell) Y_{SHB}\, V_3$

The above equations are "qudratized", i.e. with the addition of new variables, the equations are expressed in terms of linear terms and few quadratic terms. The final result includes the following state vector.

$x^T = [V_1, V_2, \ell, g, | V_3, x, y]$

and the measurement vector is:

$z_1^T = [I_1^m, I_2^m, V_1^m, V_2^m, g, V_{n1}, V_{n2}]$

3.3.2 Matrix Formulation

The state vector is partitioned as follows:

$x_1^T = [V_1, V_2, \ell, g, a_i]$, and $x_2^T = [V_3, x, y, y_a, y_b, a_r]$

Define the measurement vector z as follows:

$z^T = [I_1^m, I_2^m, V_1^m, V_2^m, V_{n1}, V_{n2}, g, a_r]$

Using the above state and measurement vector definitions, the linearized system of cat equations (7) is written in compact arf matrix notation as follows:

$z = H_1 x_1 + H_2 x_2 - b + r$

$0 = K_1 x_1 + K_2 x_2 - c$

The optimization solution is computed as follows. Solving constraint equation for x2:

$x_2 = K_2^{-1} (c - K_1 x_1)$

Substituting x2 in the measurement equation and manipulating:

$z = (H_1 - H_2 K_2^{-1} K_1) x_1 + H_2 K_2^{-1} c - b + r$

let $H = H_1 - H_2 K_2^{-1} K_1$,
and $d = z + b - H_2 K_2^{-1} c$

then the optimization result is:

$x_1 = (H^T WH)^{-1} H^T W d$
$x_2 = K_2^{-1} (c - K_1 x_1)$

3.3.3 Solution Algorithm

The Solution algorithm is as follows:

1. Compute approximate solution using method described in section 3.1
2. Compute Matrices H1, H2, K1, K2, and Vectors b and c at operating point.
3. Update states x_1, x_2 as follows:

   $x_1 = (H^T WH)^{-1} H^T W d$
   $x_2 = K_2^{-1} (c - K_1 x_1)$
   where:
   $H = H_1 - H_2 K_2^{-1} K_1$
   $d = z + b - H_2 K_2^{-1} c$

4. Compute Residual Norm oink ρ as follows:
   $\rho = || z + b - H_1 x_1 - H_2 x_2 ||$ and if $\Delta\rho < \varepsilon_1$ Stop, otherwise go to step 2.

3.3.4 Simulation of Asymmetry, Grounding and Arc Effects

The described model can be used to evaluate the impact of asymmetry, grounding and arc effects on the accuracy of fault locating. For this purpose, the model described above can be "forced" to (a) ignore asymmetry, (b) ignore grounding, (c) ignore the arc voltage or any combination of the above. For example, in order to ignore the arc voltage it is sufficient to set the variable g equal to zero. In order to ignore the transmission tower grounds it is sufficient to set the tower grounds equal to a small value, i.e. 0.1 ohms. Or in order to ignore asymmetry, the line matrices are computed from the positive, negative and zero sequence impedances.

4.0 Implementation and Numerical Experiments

The proposed algorithm has been implemented in the XFM program. XFM is a general purpose data analysis program with the capability to exchange data using the COMTRADE format. The proposed fault distance estimation algorithms have been implemented in this program.

Data for numerical experiments of the proposed fault locating algorithms were generated using a time domain simulation program (WinIGS-T). WinIGS-T is a general-purpose transient analysis program employing physically based models of power system components (sources, transmission lines, loads etc). The user interface of this program is illustrated in Figure 5, showing a single line diagram of the network that was used to generate the fault test data, as well as a selection of the generated waveforms. Note that an arc model is included which represents the nonlinear fault arc characteristics (see bottom waveform in Figure 5).

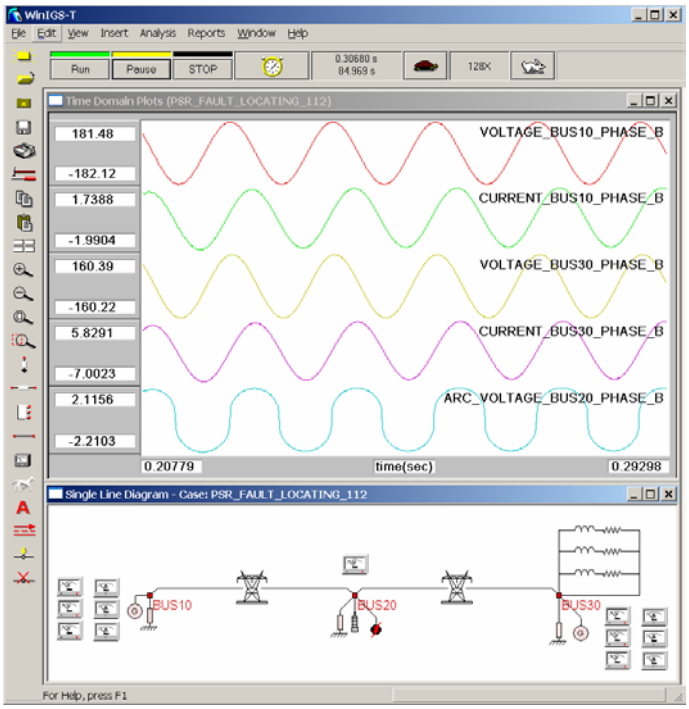

Figure 5. WinIGS-T User Interface

The generated voltage and current waveforms at the transmission line end terminals are transferred to the XFM program and used as input for the fault location algorithms. The data transfer is accomplished via COMTRADE files.

The user interface of the XFM program is illustrated in Figure 6. Note that the faulted circuit parameters can be defined in two ways: (a) by inputting the positive, negative and zero sequence parameters of the circuit as it is illustrated in the upper left corner of the user interface window, or (b) by entering the physical data of the circuit, such as tower configuration, phase conductors, shield/neutral conductors, tower ground impedance, etc.

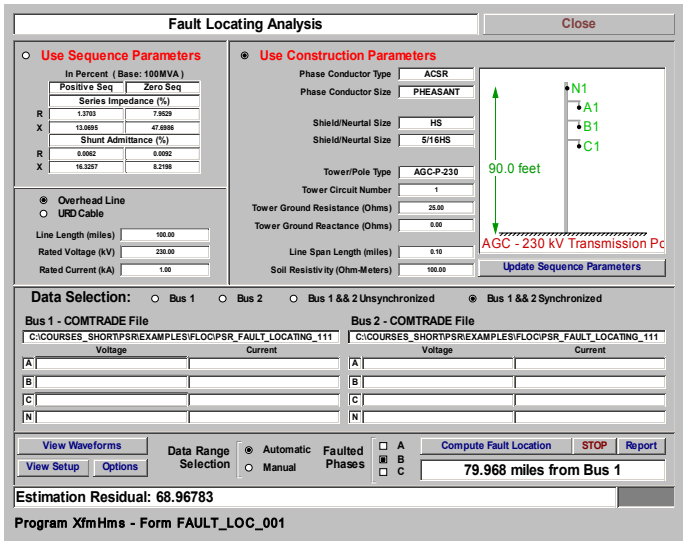

(a)

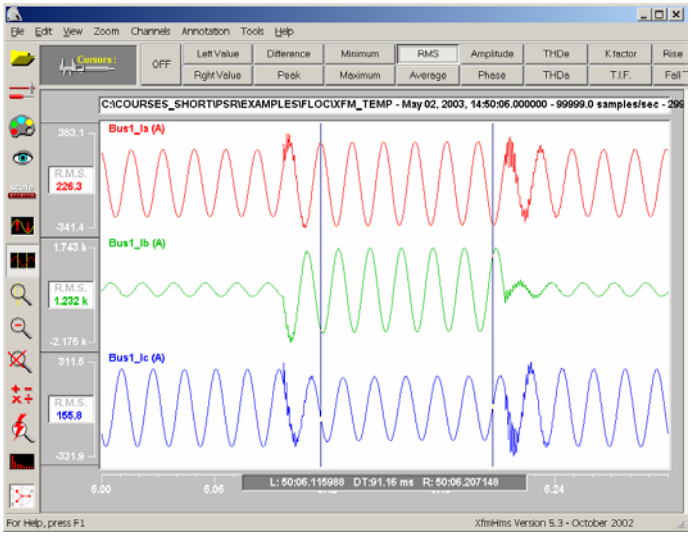

(b)

Figure 6. XFM User Interface
(a) Parameter Entry, (b) Waveform Display

Irrespectively of the type of data specified, the algorithm computes the resistance, inductance and capacitance of the circuit per unit length (as a matter of fact, these parameters are matrices). It should be apparent that if the sequence parameters are specified, the computed resistance, inductance and capacitance of the circuit are approximations of the actual parameters [9]. The next step is to specify the location of the recorded data. For this purpose, it is assumed that the data reside in a data file in COMTRADE format. The user can navigate to specify the specific COMTRADE file and then the appropriate channels from the file are selected. This is shown in the lower part of the user interface window. Note that depending on the available data, the user may select single-end data, two-end synchronized data, or two-end non-synchronized data.

The COMTRADE data are processed by the proposed algorithms. When the full model is used (asymmetric transmission line model, grounding impedances, arc voltage, etc), the fault location is precisely computed. This is so because the system does not include the errors resulting from instrumentation errors. Then the fault locating algorithms are repeated with different approximate models, for example, in order to neglect asymmetry, the impedance matrices of the circuit are symmetrized [10]. Then the fault locating algorithms is repeated with the symmetrized transmission line model. The results of these numerical experiments are illustrated in Table 1 for two specific lines, one with horizontal arrangements (H-Frame) and another with a vertical arrangement. The results are self explanatory. Note that the line asymmetry is by far the most important parameters for the accuracy of the fault locating algorithms. For calibration purposes, the fault location is at 20 miles, therefore a 1% error represents 0.2 miles. Note that the table lists only two end data (synchronized and unsynchronized). In the absence of instrumentation errors, the results of two end synchronized and unsynchronized data are very close. The results with single end data exhibit large errors with the approximate models. The reason for this behavior is the use of phasors for the estimation of the fault distance. The performance of the fault locating algorithm drastically improves when a dynamic estimation method is used. The dynamic estimation method has been presented in an earlier paper [14]. The results of this method are not presented here since that will not provide a valid comparison (comparison of static and dynamic estimation method).

6.0 Summary

Comprehensive fault distance estimation algorithms have been presented based on detailed faulted circuit models. The algorithms have been used in numerical experiments to quantify the effect of various approximations of the faulted circuit model on the accuracy of the fault distance estimation. From the approximations considered, the faulted circuit asymmetry has the largest impact. Numerical experiments will be continued to evaluate other sources of error.

References

1. A. P. Sakis Meliopoulos, G. J. Cokkinides and Jay Murphy, “Use of DFR Data for Fault Locating”, *Proceedings of the 2000 Georgia Tech Fault and Disturbance Analysis Conference*, Atlanta, Georgia, May 4-5, 2000.
2. A. P. Sakis Meliopoulos, G. J. Cokkinides and R. I. James, “Transformer Diagnostic System for Loss of Life and Coil Integrity”, *Proceedings of the 1998 Georgia Tech Fault and Disturbance Analysis Conference*, Atlanta, Georgia, May 4-5, 1998.
3. D. L. Waikar, A. C. Liew, and S. Elangovan, “Design, Implementation and Performance Evaluation of a New Digital Distance Relaying Algorithm”, IEEE Transactions on Power Systems, Vol. 11, No. 1, pp. 448-456, February 1996.
4. L. Eriksson, M. M. Saha, and G. D. Rockefeller, “An Accurate Fault Locator with Compensation for Apparent Reactance in the Fault Resistance Resulting from Remote-End Infeed”, IEEE Transactions on Power Apparatus and

Systems, Volume PAS-104, No. 2, pp. 424-436, February 1985.
5. H. Y. Li, E. P. Southern, P. A. Crossley, S. Potts, S. D. A. Pickering, B. R. J. Caunce, and G. C. Weller, "A New Type of Differential Feeder Protection Relay Using the Global Positioning System for Data Synchronization", IEEE Transactions on Power Delivery, Vol. 12, No. 3, pp. 1090-1097, July 1997.
6. W. Peterson, D. Novosel, D. Hart, T. W. Cease and J. Schneider, "Tapping IED Data to Find Transmission Faults", IEEE Computer Applications in Power, pp. 36-42, April 1999.
7. D. Novosel, D. G. Hart, E. Udren, and J. Garrity, "Unsynchronized Two-Terminal Fault Location Estimation", IEEE Transactions on Power Delivery, Vol. 11, No. 1, pp. 130-136, January 1996.
8. E. J. Bartlett, and P. J. Moore, "Detection and Analysis of Power System Transient Induced VHF Electromagnetic Radiation for Arcing Fault Location", Proceeding of the IASTED International Conference, pp 305-320, November 8-10, 1999.
9. M. Kezunovic and B. Perunicic, "Automated Transmission Line Fault Analysis Using Synchronized Sampling at Two Ends", IEEE Transactions on Power Systems, Vol. 11, No. 1, pp. 441-447, February 1996.
10. A. P. Sakis Meliopoulos, Power System Grounding and Transients, Marcel Dekker Inc., 1988.
11. A. P. Meliopoulos, F. Zhang, S. Zelingher, G. Stillmam, G. J. Cokkinides, L. Coffeen, R. Burnett, J. McBride, "Transmission Level Instrument Transformers and Transient Event Recorders Characterization for Harmonic Measurements", IEEE Transactions on Power Delivery, Vol. 8, No. 3, pp. 1507-1517, July 1993.
12. A. R. Warrington, *Protective Relays, their Theory and Practice, Volume 1*, Chapman and Hall Ltd., London, 1968.
13. A. R. Warrington, *Reactance Relays Negligibly Affected by Arc Impedance*, Electrical World, pp. 502-505, September 1931.
14. A. P. Sakis Meliopoulos and George J. Cokkinides, "Visualization and Animation of Protective Relays Operation from DFR Data" Proceedings of the 2001 Georgia Tech Fault and Disturbance Analysis Conference, Atlanta, Georgia, April 30-May 1, 2001.

BIOGHRAPHIES

A. P. Sakis Meliopoulos (M '76, SM '83, F '93) was born in Katerini, Greece, in 1949. He received the M.E. and E.E. diploma from the National Technical University of Athens, Greece, in 1972; the M.S.E.E. and Ph.D. degrees from the Georgia Institute of Technology in 1974 and 1976, respectively. In 1971, he worked for Western Electric in Atlanta, Georgia. In 1976, he joined the Faculty of Electrical Engineering, Georgia Institute of Technology, where he is presently a professor. He is active in teaching and research in the general areas of modeling, analysis, and control of power systems. He has made significant contributions to power system grounding, harmonics, and reliability assessment of power systems. He is the author of the books, *Power Systems Grounding and Transients*, Marcel Dekker, June 1988, *Ligthning and Overvoltage Protection*, Section 27, Standard Handbook for Electrical Engineers, McGraw Hill, 1993. He holds three patents and he has published over 180 technical papers. Dr. Meliopoulos is the Chairman of the Georgia Tech Protective Relaying Conference, a Fellow of the IEEE and a member of Sigma Xi.

George Cokkinides (M '85) was born in Athens, Greece, in 1955. He obtained the B.S., M.S., and Ph.D. degrees at the Georgia Institute of Technology in 1978, 1980, and 1985, respectively. From 1983 to 1985, he was a research engineer at the Georgia Tech Research Institute. Since 1985, he has been with the University of South Carolina where he is presently an Associate Professor of Electrical Engineering. His research interests include power system modeling and simulation, power electronics applications, power system harmonics, and measurement instrumentation. Dr. Cokkinides is a member of the IEEE/PES.

Table 1. Typical Numerical Experiment Results

				%Error (of fault distance computation)		
Case Code	**Phase Conductor Arrange-ment**	**Tower Grounding Resistance (Ohms)**	**Arc Voltage (kV)**	**Computed Distance Neglecting Asymmetry**	**Computed Distance Neglecting Tower Ground Resistance**	**Computed Distance Neglecting Arc Voltage**
111	Vertical	25	0	-0.92	0.0015	
112	Vertical	25	2	-0.80	0.0015	0.0005
121	Vertical	50	0	-1.02	0.0015	
122	Vertical	50	2	-1.05	0.0015	0.0005
131	Vertical	100	0	-1.15	0.0025	
132	Vertical	100	2	-1.18	0.0025	0.0005
211	Horizontal	25	0	-1.21	0.0015	
212	Horizontal	25	2	-1.21	0.0015	0.0000
221	Horizontal	50	0	-1.20	0.0020	
222	Horizontal	50	2	-1.19	0.0020	0.0000
231	Horizontal	100	0	-1.18	0.0025	
232	Horizontal	100	2	-1.17	0.0025	-0.0005